JCI insight

Targetable purinergic receptors $P2Y_{12}$ and A2b antagonistically regulate bladder function

Yuan Hao, … , Mark L. Zeidel, Weiqun Yu

JCI Insight. 2019;4(16):e122112. https://doi.org/10.1172/jci.insight.122112.

Research Article **Aging** **Muscle biology**

Abnormalities in purine availability or purinergic receptor density are commonly seen in patients with lower urinary tract symptoms (LUTS), but the underlying mechanisms relating altered receptor function to LUTS are unknown. Here we provide extensive evidence for the reciprocal interplay of multiple receptors responding to ATP, ADP (adenosine diphosphate), and adenosine, agonists that regulate bladder function significantly. ADP stimulated $P2Y_{12}$ receptors, causing bladder smooth muscle (BSM) contraction, whereas adenosine signaling through potentially newly defined A2b receptors, actively inhibited BSM purinergic contractility. The modulation of adenylyl cyclase-cAMP signaling via A2b and $P2Y_{12}$ interaction actively regulated bladder contractility by modulating intracellular calcium levels. KO mice lacking the receptors display diametrically opposed bladder phenotypes, with $P2Y_{12}$-KO mice exhibiting an underactive bladder (UAB) phenotype with increased bladder capacity and reduced voiding frequency, whereas A2b-KO mice have an overactive bladder (OAB), with decreased capacity and increased voiding frequency. The opposing phenotypes in $P2Y_{12}$-KO and A2b-KO mice not only resulted from dysregulated BSM contractility, but also from abnormal BSM cell growth. Finally, we demonstrate that i.p. administration of drugs targeting $P2Y_{12}$ or A2b receptor rescues these abnormal phenotypes in both KO mice. These findings strongly indicate that $P2Y_{12}$ and A2b receptors are attractive therapeutic targets for human patients with LUTS.

JCI insight

RESEARCH ARTICLE

Targetable purinergic receptors $P2Y_{12}$ and A2b antagonistically regulate bladder function

Yuan Hao,[1] Lu Wang,[1,2] Huan Chen,[1] Warren G. Hill,[1] Simon C. Robson,[1] Mark L. Zeidel,[1] and Weiqun Yu[1]

[1]Department of Medicine, Beth Israel Deaconess Medical Center and Harvard Medical School, Boston, Massachusetts, USA. [2]Chongqing University, Chongqing, China.

Abnormalities in purine availability or purinergic receptor density are commonly seen in patients with lower urinary tract symptoms (LUTS), but the underlying mechanisms relating altered receptor function to LUTS are unknown. Here we provide extensive evidence for the reciprocal interplay of multiple receptors responding to ATP, ADP (adenosine diphosphate), and adenosine, agonists that regulate bladder function significantly. ADP stimulated $P2Y_{12}$ receptors, causing bladder smooth muscle (BSM) contraction, whereas adenosine signaling through potentially newly defined A2b receptors, actively inhibited BSM purinergic contractility. The modulation of adenylyl cyclase-cAMP signaling via A2b and $P2Y_{12}$ interaction actively regulated bladder contractility by modulating intracellular calcium levels. KO mice lacking the receptors display diametrically opposed bladder phenotypes, with $P2Y_{12}$-KO mice exhibiting an underactive bladder (UAB) phenotype with increased bladder capacity and reduced voiding frequency, whereas A2b-KO mice have an overactive bladder (OAB), with decreased capacity and increased voiding frequency. The opposing phenotypes in $P2Y_{12}$-KO and A2b-KO mice not only resulted from dysregulated BSM contractility, but also from abnormal BSM cell growth. Finally, we demonstrate that i.p. administration of drugs targeting $P2Y_{12}$ or A2b receptor rescues these abnormal phenotypes in both KO mice. These findings strongly indicate that $P2Y_{12}$ and A2b receptors are attractive therapeutic targets for human patients with LUTS.

Introduction

Lower urinary tract symptoms (LUTS) constitute a group of urinary disorders that are highly prevalent and affect more than half of the population aged older than 40 years (1, 2). Current drugs for LUTS include antimuscarinics and a recent FDA-approved agonist targeting adrenergic β_3 receptors in bladder smooth muscle (BSM). Because these drugs have limited efficacy and high rates of adverse effects, they are often discontinued by patients (3–5). For example, oxybutynin, an antimuscarinic drug targeted to treat bladder overactivity (OAB), shows marginal beneficial effects of only 13%–25% over placebo (5), and a study in rats indicated that chronic administration of oxybutynin induced a shift from muscarinic to purinergic transmission in the bladder wall. This finding, if also true in humans, indicates a likely reduction in antimuscarinic efficacy with prolonged treatment (6). Therefore, there is a clear need to identify new pathways and better targets for treating LUTS.

The urinary bladder undergoes multiple cycles of filling and emptying each day, which requires coordinated BSM contraction and relaxation. Accordingly, regulation of BSM contraction and relaxation is critical for normal bladder function. The contraction stimulus that leads to voiding is initiated by firing of parasympathetic motor neurons that release neurotransmitters acetylcholine and ATP. Acetylcholine binds to muscarinic receptors M2 and M3, and ATP binds to purinergic receptor $P2X_1$ (7–9). Although purinergic signaling is accepted to be prominent in rodents, its role in human bladder physiology is controversial, with many clinicians believing its contribution to be minimal. This belief arises from experiments showing that atropine, a muscarinic antagonist, blocks approximately 95% of nerve-mediated BSM contraction when stimulated by electrical field stimulation (EFS). However, other studies suggest a far more important role for purinergic signaling. For example, it has been shown that the neuromuscular purinergic component in human female bladders and in the bladder trigone accounts for about 50% and 40% of nerve-mediated

Authorship note: YH and LW contributed equally.

Conflict of interest: The authors have declared that no conflict of interest exists.

Submitted: May 22, 2018
Accepted: July 26, 2019
Published: August 22, 2019.

Reference information: *JCI Insight*. 2019;4(16):e122112. https://doi.org/10.1172/jci.insight.122112.

contraction force, respectively (10, 11). In addition, externally applied α,β-meATP (as opposed to EFS-stimulated neuronal release) elicited significant human BSM contraction, and $P2X_1$ receptor is highly expressed in human BSM (12, 13). In pathological conditions, contraction in response to neuromuscular purinergic signaling can account for up to 65% of total force in patients with OAB, partial bladder outlet obstruction, and diabetic bladder dysfunction (14–19). A common finding in these patients is elevated ATP release and/or altered P2X receptor expression. Finally, the importance of purinergic signaling in regulating bladder function is further confirmed by recent findings from 2 human patients with loss-of-function mutations in ENTPD1, an ectonucleotidase enzyme that converts ATP to ADP and ADP to AMP (20). These patients display bladder hypomotility and incontinence (Alexander Lossos, personal communication).

Intriguingly, bladder myocytes express ENTPD1 and ecto-5′-nucleotidase (NT5E) on their cell surface (21), meaning that ATP is eventually converted into ADP and ultimately adenosine by these enzymes. Both compounds have been shown to have bioeffector functions on BSM. ADP was reported to be a potent agonist for inducing BSM contraction, and ADPβS (an analog of ADP) was found to be as potent as $P2X_1$ receptor agonist α,β-meATP in inducing human BSM contraction (12, 22, 23). Using pharmacological tools, we recently demonstrated that ADP-induced bladder contractility is mediated by $P2Y_{12}$ receptor and that contraction was temporally regulated by ectonucleotidases and adenosine signaling (24). Adenosine, which originated from the conversion of ADP by Nt5E, was reported to relax BSM by activating adenosine A2 receptors. Both A2a and A2b have been suggested as being expressed in BSM for bladder relaxation (25–28); however, the exact adenosine receptor subtypes and how they are involved in modulating bladder activity has remained unclear.

It thus appears that all the necessary machinery exists for ATP and its downstream metabolites, ADP and adenosine, to play an important functional role in regulating bladder activity. In addition, the purinergic receptors mediating the effects of these signaling molecules could be druggable targets for treating bladder dysfunctions. However, how these molecules and receptors regulate contraction and relaxation, and whether these signaling cascades have coordinated interplay, remains unknown. To answer these questions, we have investigated in vivo and in vitro bladder function in both $P2Y_{12}$ and A2b receptor–KO mice. Our data indicate that these receptors signal in opposing directions through modulation of adenylyl cyclase and cyclic AMP (AC-cAMP) pathway in a way that has effects on calcium signaling. Notably, in vivo administration of compounds that target these 2 receptors rescues phenotypic abnormalities in both models.

Results

Activation of adenosine A2 receptors predominantly inhibits purinergic, but not muscarinic, BSM contraction. Adenosine or adenosine receptor agonists are known to relax BSM contraction through the activation of A2 receptors. To explore the underlying mechanism, we tested this effect by using a nonselective adenosine agonist NECA in mucosa-dissected mouse BSM strips. Myography indicates that NECA significantly inhibited EFS-induced BSM contraction, especially at low-frequency EFS stimulation, which abolished most of the force (Figure 1A, left-hand contraction spikes). However, NECA did not inhibit BSM contraction completely, which was evident at higher frequency EFS stimulation (Figure 1A, right-hand spikes), in which approximately 60% of the force remains even at high doses.

It has been suggested that BSM purinergic contractility is sensitive to low-frequency EFS stimulation which functions to initiate BSM contraction, whereas BSM muscarinic contractility is sensitive to high-frequency EFS stimulation, which functions to produce sustained BSM contraction to expel urine (8). Based on results seen in Figure 1A, in which the degree of inhibition was dependent on electrical field frequency, we hypothesized that NECA might predominantly inhibit BSM purinergic contractility. To test this hypothesis, we pretreated the BSM with 0.5 μM atropine, which abolished the muscarinic contractility and spared purinergic contractility. In this condition, further treatment of BSM with NECA completely inhibited BSM contractility with an IC_{50} of approximately 0.53 μM (Figure 1, B, D, and E), supporting our hypothesis. Conversely, pretreatment of BSM with α,β-meATP, which desensitizes a major BSM purinergic receptor $P2X_1$, revealed that α,β-meATP-resistant force was largely insensitive to NECA (Figure 1, C and E) but could be completely abolished by further atropine treatment (data not shown). These data clearly indicate that adenosine receptor activation in BSM by NECA predominantly inhibits BSM contraction driven by purinergic agonists (we define this as purinergic contraction). We further tested whether activation of adenosine receptor inhibits ADP-mediated BSM contraction. NECA dose-dependently abolished ADPβS-elicited BSM contraction (Figure 1, F and G), suggesting there is elaborate interplay among ATP, ADP, and adenosine-mediated signaling in regulating bladder contractility.

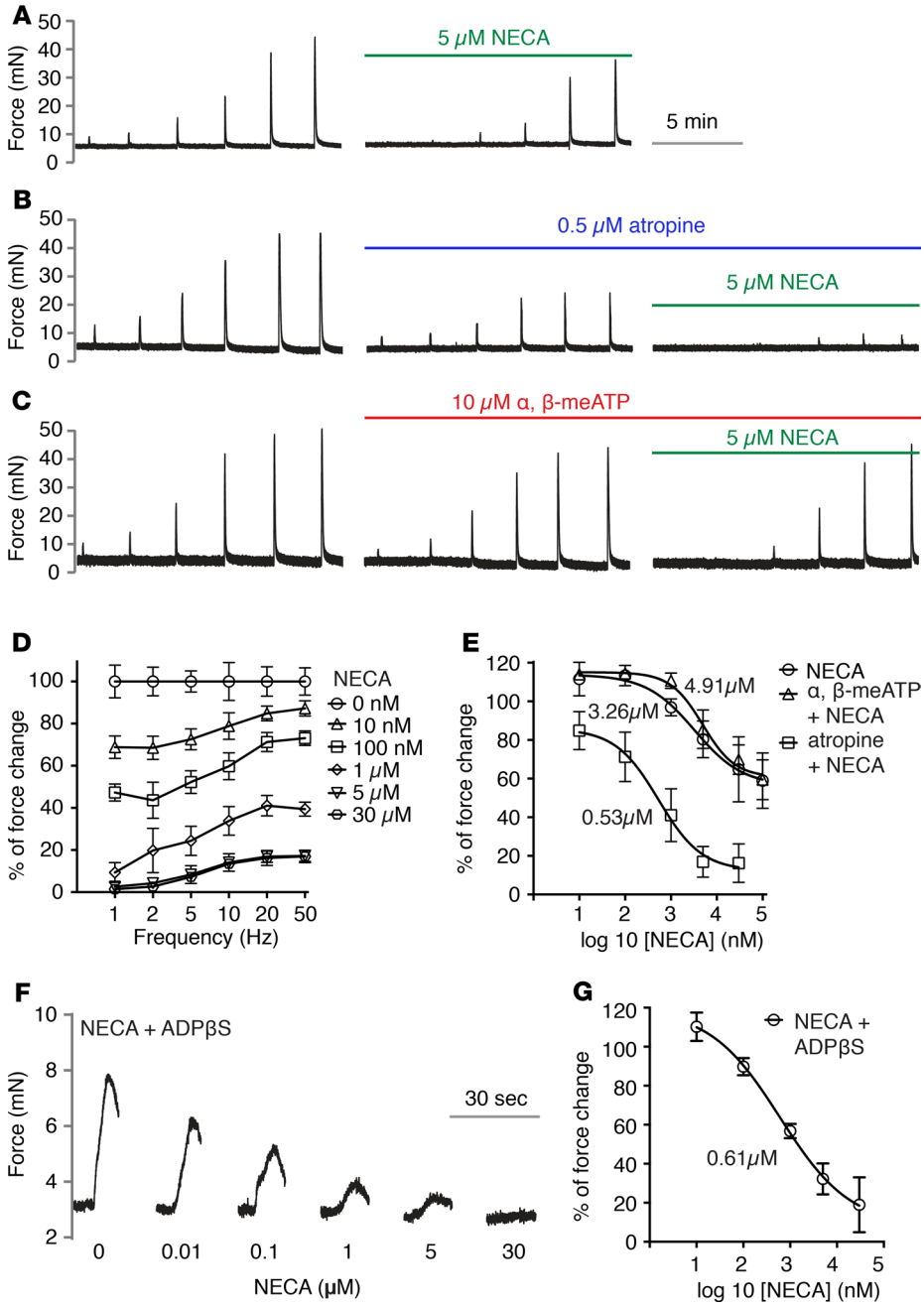

Figure 1. Activation of adenosine receptor inhibits bladder smooth muscle purinergic contraction. Bladder smooth muscle (BSM) strips were stimulated by electrical field stimulation (EFS) at indicated frequencies in increasing order (**D**: *x*-axis). (**A**) Representative traces of BSM contraction in response to EFS stimulation, which is partially inhibited by 10 minutes NECA pretreatment (n = 10). The EFS frequencies used are shown on the *x*-axis in **D**. (**B**) Pretreatment with atropine inhibits muscarinic contraction, and the remaining purinergic contraction (or atropine resistant) is fully inhibited by NECA (n = 8). (**C**) When ATP-mediated purinergic contraction is inhibited by α,β-meATP desensitization, the remaining muscarinic contraction is not sensitive to NECA activation of adenosine receptor (n = 8). Force changes were normalized to control and shown as percentages. (**D**) Quantitation of data shown in **B**. (**E**) Nonlinear regression of **A**, **B**, and **C**, which shows the dose response under 20-Hz EFS stimulation, and the corresponding IC_{50}. (**F**) Representative traces of BSM contraction in response to ADPβS (n = 7), which is dose-dependently inhibited by NECA pretreatment. Quantitation shown in **G**. Data are shown as mean ± SD, dose response was analyzed by 1-way ANOVA, $P < 0.05$

A2b is the major adenosine receptor mediating inhibition of BSM purinergic contraction. To determine which A2 receptor mediates purinergic inhibition, we tested the effect of potent A2a- and A2b-selective receptor agonists, CGS21680 and Bay 60-6583, respectively. At concentrations known to inhibit selectively A2b receptors, Bay 60-6583 dose-dependently inhibits EFS-induced BSM contraction. The observed IC_{50} of approximately 1.76 nM and near-complete inhibition of BSM purinergic contraction force at approximately 50 nM were consistent with its reported IC_{50} (Figure 2, B and G). Conversely, CGS21680 exhibited little effect, even at dosages much higher than its IC_{50} (Figure 2, A and G), suggesting that A2b is the major receptor inhibiting purinergic contraction.

In further support of our hypothesis, CGS21680 and Bay 60-6583 were tested for their ability to inhibit ATP and ADP-mediated contraction pathways induced by α,β-meATP (mediated by $P2X_1$) and ADPβS (mediated by $P2Y_{12}$). As seen in Figure 2, C–F, Bay 60-6583 potently inhibited contraction by these 2 agonists whereas the A2a agonist CGS21680 had no effect (Figure 2, C–F, H, I). Finally, the dominant role of A2b receptor was further confirmed by A2b-KO mice, in which Bay 60-6583 failed to inhibit BSM purinergic contraction (Figure 2, J–L).

Genetic deletion of A2b or $P2Y_{12}$ receptor results in altered conscious voiding patterns and urodynamic parameters. To understand the in vivo function of A2b receptor and $P2Y_{12}$ receptor-mediated signaling, $P2Y_{12}$-KO and A2b-KO mice were examined. Deletion of $P2Y_{12}$ and A2b genes were verified by genomic DNA genotyping (Supplemental Figure 1, A and C; supplemental material available online with this article; https://doi.org/10.1172/jci.insight.122112DS1) and mRNA expression analysis (Supplemental Figure 1, B and D). A2b gene KO was further determined using X-gal staining, with which β-gal (knocked into A2b-KO mice) can be visualized in blue (Supplemental Figure 1E).

Interestingly, deletion of $P2Y_{12}$ resulted in a significantly heavier bladder. In direct contrast, deletion of A2b resulted in a significantly smaller and lighter bladder (Table 1). To evaluate conscious spontaneous bladder function in these KO mice, quantitative voiding spot assays (VSAs) were performed in female mice. As shown in Figure 3, A–F, normal wild-type mice produced approximately 3.80 primary voiding spots (PVSs) of 346 mm^2 mean area in a 4-hour period. Deletion of $P2Y_{12}$, however, resulted in significantly larger PVSs but there were fewer of them, whereas deletion of A2b caused significantly smaller spots with increased numbers of individual voids (Figure 3, A–F). Because of the potential differences of purinergic signaling in male and female mice bladders, VSAs were also performed in male $P2Y_{12}$ and A2b KO mice. Consistently, similar phenotypes were observed (Supplemental Figure 2). Thus, deletion of $P2Y_{12}$ resulted in reduced voiding frequency and large bladder capacity, and deletion of A2b receptor created the opposite phenotype with increased voiding frequency and a smaller bladder capacity.

Bladder urodynamic function of $P2Y_{12}$-KO and A2b-KO mice was next characterized by cystometrogram (CMG) in female mice. Figure 3, G–I, shows CMG traces in which time-dependent bladder pressure changes are recorded during continuous filling and emptying cycles, from wild-type mice and both KO models. Intrabladder pressure profiles were dramatically different between models, with $P2Y_{12}$-KO mice having much longer intercontractile (voiding) intervals than wild-type mice, whereas compliance was greater and micturition pressures (i.e., peak pressure) were higher (Figure 3, J–N). Diametrically opposed to this, the A2b-KO mice exhibited significantly shorter intercontractile intervals, reduced bladder compliance, and lower micturition pressures than wild-type mice (Figure 3, J–N). Basal pressure and threshold pressure (for voiding) were not different, suggesting that there was no afferent sensory defect in the KO mice. These altered urodynamics are fully consistent with the bladder morphology and VSA data and, in sum, indicate that $P2Y_{12}$-KO mice have a UAB phenotype, whereas the A2b-KO mice exhibit an OAB phenotype. Collectively, these observations suggest critical roles for $P2Y_{12}$ and A2b signaling in regulating bladder activity and further indicate the importance of extracellular ATP, ADP, and adenosine kinetics for bladder smooth muscle function.

Deletion of A2b or $P2Y_{12}$ receptor affects BSM contraction force in opposing directions. To determine whether loss of these receptors affects BSM contractility, which might explain the bladder phenotypes observed previously, we performed myography on isolated BSM strips. As shown in Figure 4A, normal BSM contractile force increased with increasing of EFS frequency, and average maximum force reaches approximately 30 mN. Deletion of $P2Y_{12}$ resulted in BSM that contracts more strongly, with the maximum force approaching 50 mN. In contrast, deletion of A2b receptor significantly reduces BSM contractile force, with maximum force only reaching approximately 20 mN (Figure 4, A–D). By pretreating BSM tissue with atropine to block muscarinic contractile force, we investigated whether deletion of A2b or $P2Y_{12}$ affects the purinergic

Table 1. Deletion of $P2Y_{12}$ (n = 8) or A2b (n = 10) receptor results in altered bladder weights

	Wild-type (n = 9)	$P2Y_{12}$-KO (n = 8)	A2b-KO (n = 10)
Body weight (g)	26.23 ± 1.36	29.50 ± 1.31	25.50 ± 0.81
Bladder weight (mg)	26.18 ± 1.89	40.61 ± 2.42*	20.60 ± 1.07*
Bladder/body (mg/g)	0.99 ± 0.04	1.38 ± 0.05*	0.81 ± 0.03*

Data are shown as mean and SD, Student's t test is used to compare between wild-type and knock-out animals; *$P < 0.05$.

force component (Figure 4E). In this setting, deletion of $P2Y_{12}$ did not change the purinergic force percentage significantly; however, in A2b-deleted mice BSM, the purinergic force component increased significantly at the highest frequencies (Figure 4E).

AC-cAMP signaling cascade is critical in regulating BSM purinergic contractility through modulation of downstream Ca^{2+} signaling. $P2Y_{12}$ and A2b receptors are both G protein–coupled receptors. $P2Y_{12}$ is coupled to G_i, which inhibits adenylyl cyclase (AC) activity and thus decreases intracellular secondary messenger, cyclic AMP (cAMP). In contrast, A2b is coupled to G_S, which stimulates AC activity and increases cAMP. Logically, it appears that interplay between $P2Y_{12}$ and A2b receptors by modulating downstream AC-cAMP signaling is critical in regulating BSM purinergic contractility; this finding also explains the opposing bladder activities (VSA, CMG) and BSM contractility observed in $P2Y_{12}$-KO and A2b-KO mice.

To test whether BSM purinergic contractility is sensitive to AC-cAMP signaling, BSM was pretreated with AC activators forskolin and NKH 477 before EFS stimulation. Both forskolin and NKH 477 dose-dependently inhibited BSM purinergic contractile force (Figure 4, F–J). These data strongly suggest that AC-cAMP signaling plays a critical role in mediating the opposing effects generated by ADP and adenosine signaling via $P2Y_{12}$ and A2b, respectively.

Activation of P2X1 by ATP can stimulate BSM purinergic contraction by ryanodine receptor-mediated Ca^{2+} release (9), and our data indicate that $P2Y_{12}$ or A2b activation regulates BSM purinergic contractility by modulating AC-cAMP signaling. Thus, we hypothesized that AC-cAMP signaling could affect purinergic contractility through modulating downstream Ca^{2+} signaling. To test this hypothesis, primary cultured mouse BSM cells were used for Ca^{2+} imaging. As shown in Figure 5, ATP and ADPβS were applied to activate BSM $P2X_1$ and $P2Y_{12}$ receptors, which increased intracellular Ca^{2+} signaling significantly. However, when cells were pretreated with A2b receptor agonist Bay 60-6583, the ATP and ADPβS-induced BSM intracellular Ca^{2+} signaling was dramatically inhibited. ATP and ADPβS-induced BSM intracellular Ca^{2+} signaling was also inhibited by AC-cAMP activator forskolin, again indicating that BSM purinergic contractility is regulated by AC-cAMP signaling (Figure 5, A–H). To ascertain whether these signaling pathways are also present in the human bladder, parallel studies were performed in primary cultured human BSM cells. Consistent with the mouse data, our results in human cells indicate that ATP and ADPβS both induce significant calcium influx, which is inhibited by A2b receptor agonist Bay 60-6583 and AC-cAMP activator forskolin (Figure 5, I–L). In sum, these data strongly suggest the importance of the interplay of these receptors in regulating BSM function not just in mice, but also in humans, and suggest a conserved pathway in both species.

$P2Y_{12}$ and A2b signaling modulate BSM cell growth differentially. In addition to the acute effects on BSM contractility, AC-cAMP signaling is also an important pathway in regulating cellular proliferation and differentiation by phosphorylating transcription factors, such as cyclic AMP response element (CREB) (29–32). CREB can further upregulate downstream immediate early genes (IEGs), which provide important links by which extracellular signals regulate gene transcription (33). IEGs are rapidly inducible effectors playing critical roles in regulating cellular function by regulating expression of other genes, thus modulating cell survival and plasticity, proliferation, and differentiation. *c-fos* and *c-jun* are the most extensively characterized IEGs and are sometimes described as third messengers because of their critical importance in gene regulation (34). *c-fos* and *c-jun* are upregulated in neuronal cells in response to Cav1.2 activation (35–38) and in smooth muscle cells in response to mechanical stretch (39). As noted previously (Table 1), deletion of $P2Y_{12}$ results in a significantly larger bladder whereas deletion of A2b causes a smaller bladder. The difference is visually obvious (Figure 6, A–E), implying that deletion of $P2Y_{12}$ or A2b affect BSM proliferation or differentiation because of altered AC-cAMP signaling. To test whether deletion of $P2Y_{12}$ or A2b affects cell

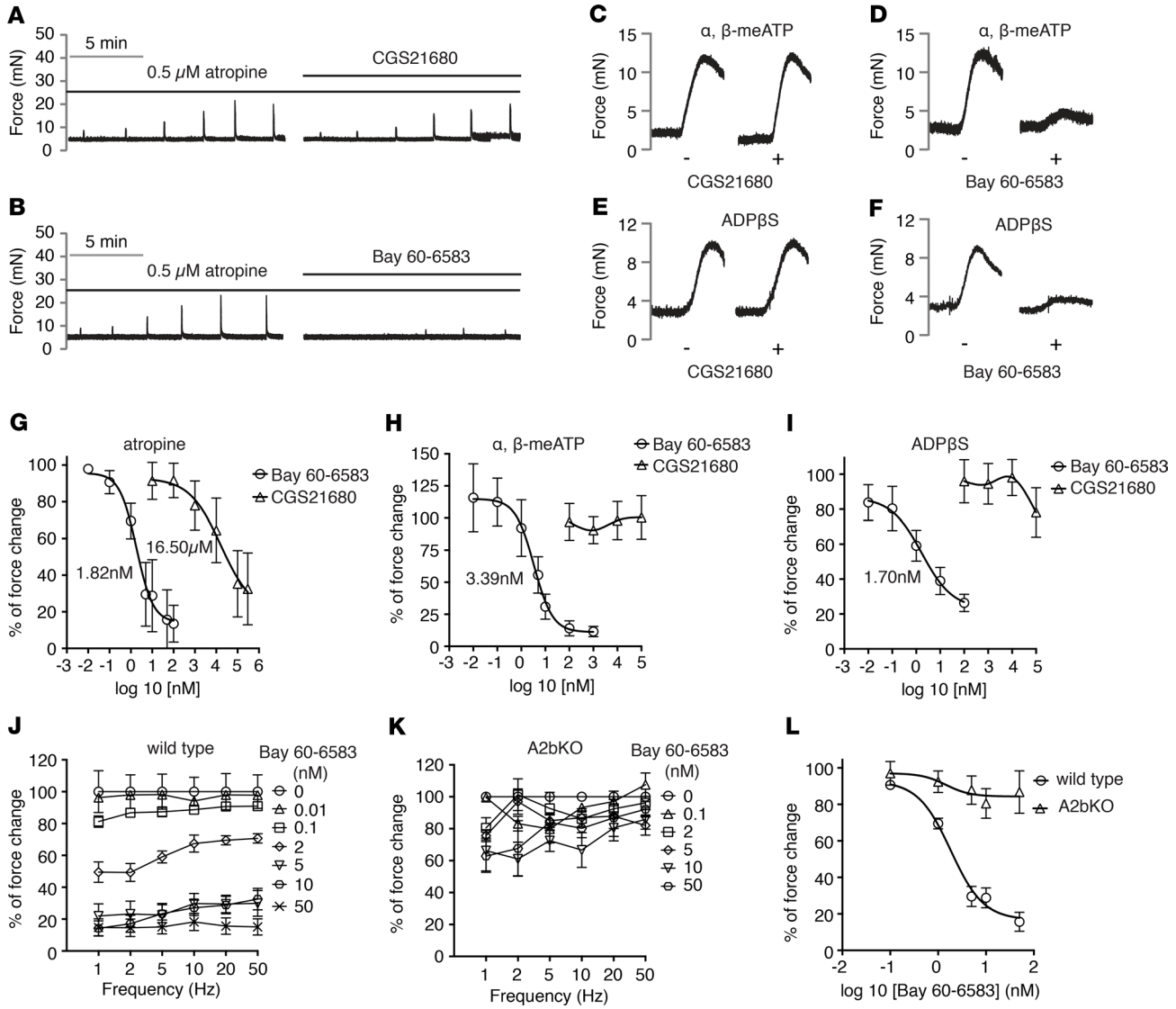

Figure 2. Adenosine A2b receptor is the major receptor in mediating inhibition of bladder smooth muscle purinergic contraction. (**A**) Representative traces of bladder smooth muscle (BSM) purinergic contraction in response to electrical field stimulation (EFS) stimulation, which is insensitive to A2a receptor activation by CGS21680 (n = 7). (**B**) Representative traces of BSM purinergic contraction in response to EFS stimulation, which can be fully inhibited by A2b receptor activation by Bay 60-6583 (n = 13). (**C**) Representative traces of BSM contraction in response to α,β-meATP stimulation, which the CGS21680 pretreatment does not inhibit (n = 7). (**D**) Pretreatment with Bay 60-6583 inhibits α,β-meATP stimulated BSM contraction (n = 7). (**E**) Representative traces of BSM contraction in response to ADPβS stimulation, which CGS21680 pretreatment does not inhibit (n = 8). (**F**) Pretreatment with Bay 60-6583 inhibits ADPβS stimulated BSM contraction (n = 7). (**G**) quantitated data of **A** and **B**. (**H**) Quantitated data of **C** and **D**. (**I**) Quantitated data of **E** and **F**. (**J**) Dose-dependent inhibition by Bay 60-6583 on BSM purinergic contraction (atropine pretreatment) in response to EFS stimulation (n = 13). This inhibition is abolished in A2b-KO BSM as shown in **K** (n = 7). (**L**) Nonlinear regression of **J** and **K**.

proliferation, sections were immunolabeled with anti-Ki67 antibody and images were quantified. The data indicated no detectable difference in the number of Ki-67$^+$ nuclei among wild-type, P2Y$_{12}$-, and A2b-deleted mice bladders (Figure 6, F–I, and Supplemental Figure 3). Interestingly, however, BSM cell size appeared to be substantially larger in P2Y$_{12}$-deleted bladders and smaller in A2b-deleted bladders (Figure 6, N and O, compared with Figure 6M). To quantitate these apparent differences, we were confronted with the problem that myocytes in any image field may be in longitudinal or transverse orientations. In addition, because they are elongated, the cross-sectional area can vary greatly depending on the position of the optical sectioning. As a result, we developed a method (shown schematically in Figure 6P) by which we only quantitated cells we viewed in cross-section (dotted rectangle) and which contained DAPI-stained nuclei. This ensured comparability of the subcellular region of similarly aligned cells for quantitative purposes. The analysis

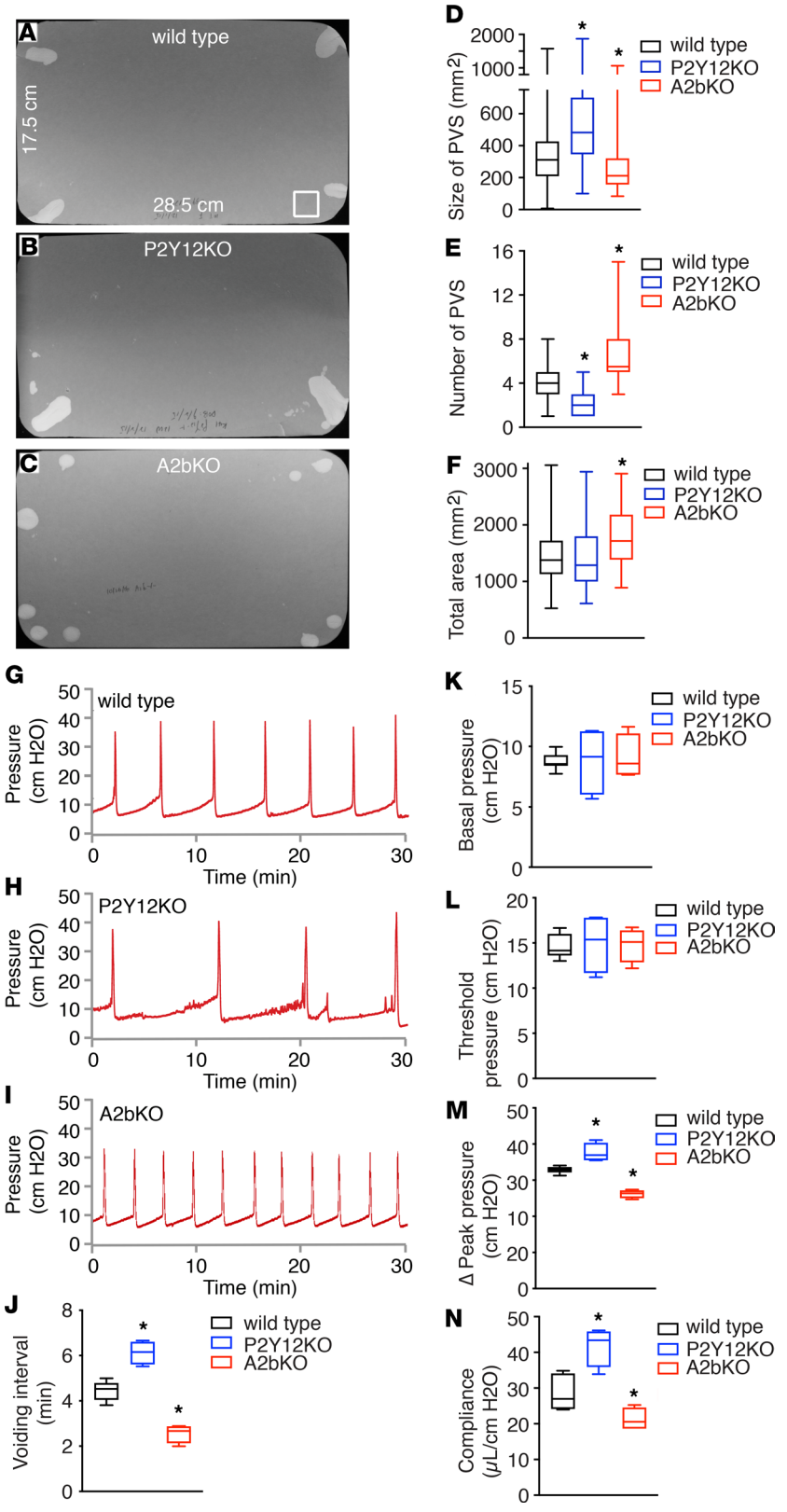

Figure 3. Deletion of $P2Y_{12}$ or A2b receptor results in altered in vivo bladder function. (**A**–**C**) are representative images of voiding spot assay (VSA) filter papers from wild-type (n = 44), $P2Y_{12}$-KO (n = 54), and A2b-KO (n = 36) mice, respectively, which are quantitated in **D**–**F**. The square at bottom right corner of **A** (surface area of 400 mm^2) serves as a size standard. Primary void spots (PVSs) are defined as spots >80 mm^2. (**G**–**I**) Representative cystometrogram (CMG) traces from wild-type (n = 8), $P2Y_{12}$-KO (n = 4), and A2b-KO (n = 4) mice, respectively, parameters from which are quantitated in **J**–**N**. Data are shown as box and whiskers, whiskers are from minimum to maximum, Student's t test is used to compare between wild-type and KO animals; *$P < 0.05$.

revealed that $P2Y_{12}$-KO myocytes were bigger than wild-type myocytes, whereas the A2bs were smaller (Figure 6Q), suggesting that deletion of $P2Y_{12}$ or A2b affects BSM cell differentiation or growth through aberrant AC-cAMP signaling. Indeed, *c-fos* and *c-jun* were upregulated significantly at both the mRNA and protein level in $P2Y_{12}$- deleted mice bladders, consistent with the larger BSM cell size and heavier bladder in $P2Y_{12}$- deleted mice (Figure 6, R–V). To investigate whether Hippo pathway (an important signaling cascade for controlling organ size) is involved in the BSM cell size difference, critical Hippo pathway genes were analyzed using quantitative RT-PCR. The data showed marginal increases in some mRNAs from $P2Y_{12}$-KO BSM tissue compared with wild-type control, suggesting in sum, the likelihood of no involvement of this pathway (Supplemental Table 1).

In further efforts to examine the molecular mechanisms underlying the significant difference in contractile forces in $P2Y_{12}$- and A2b-deficient bladders, we determined the expression of $P2X_1$ and Cav1.2 at both mRNA and protein levels. $P2X_1$ initiates bladder contraction, and $P2Y_{12}$ and A2b signaling can modulate its contractility. Cav1.2 is an essential gene for BSM and the final executor for BSM contraction via Ca^{2+} influx, which directly determines the contraction force of BSM (40). Both $P2X_1$ and Cav1.2 are expressed at normal levels, despite the changes of contractile force in $P2Y_{12}$- and A2b-deleted mice (Supplemental Figures 4 and 5). We also determined expression of sm22α, a smooth muscle differentiation marker. Again, no detectable change can be observed in either $P2Y_{12}$-KO and A2b-KO mice (Supplemental Figures 4 and 5). However, $P2Y_{12}$ was significantly increased in A2b-deleted mouse bladder, whereas A2b was significantly increased in $P2Y_{12}$-deleted mouse bladder, confirming pathway cross-talk in modulating bladder contractility and revealed for the first time in these 2 complementary models.

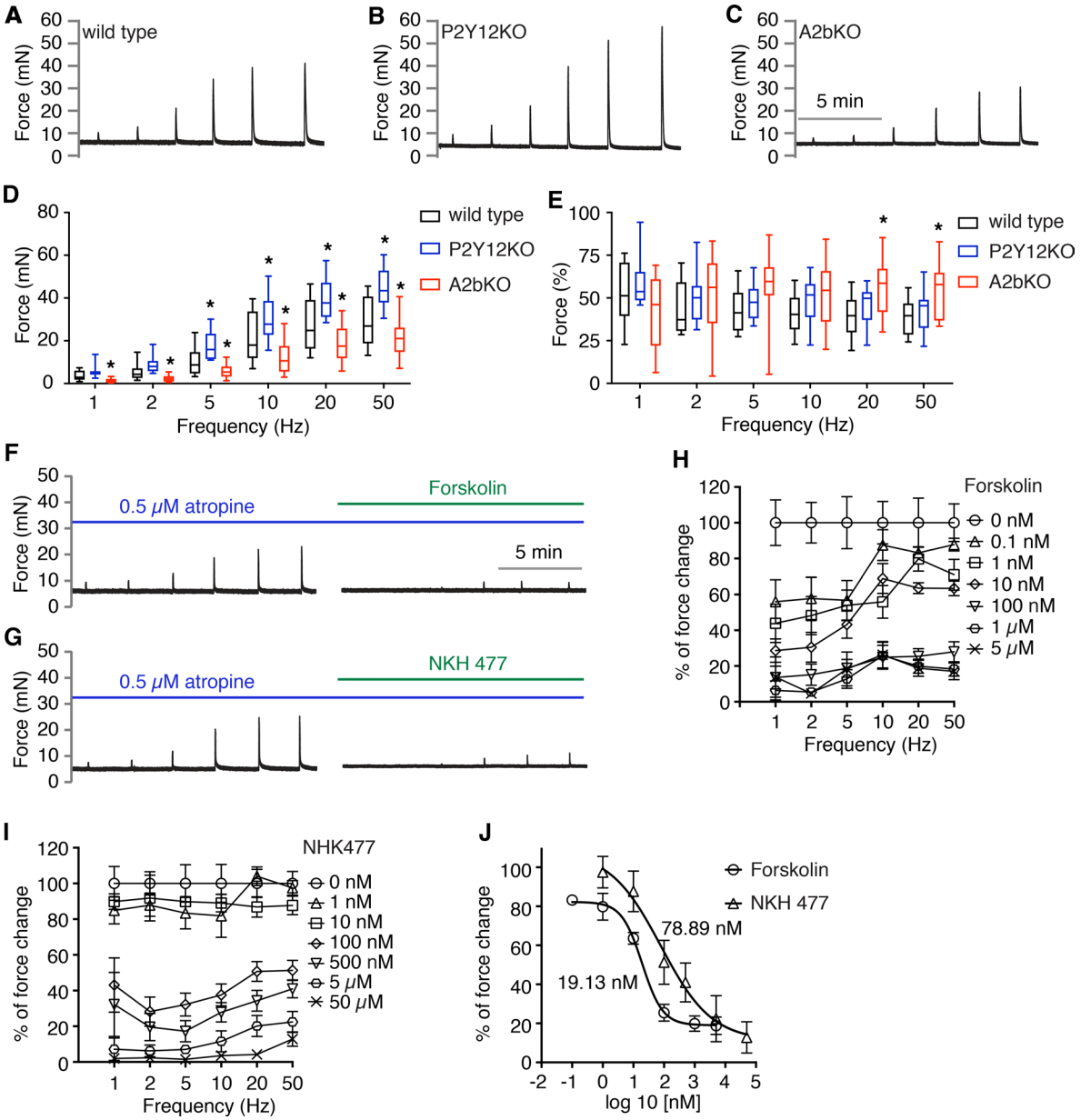

Figure 4. Deletion of $P2Y_{12}$ or A2b receptor result in altered bladder smooth muscle contractility by modulating AC-cAMP signaling. (**A**–**C**) Representative traces of bladder smooth muscle (BSM) contraction in response to electrical field stimulation (EFS) stimulation from wild-type (n = 15), $P2Y_{12}$-KO (n = 12), and A2b-KO (n = 16) mice, respectively, which are quantitated in **D**. Data are shown as box and whiskers, whiskers are from minimum to maximum, Student's t test is used to compare between wild-type and KO animals; *$P < 0.05$. (**E**) Bladder strips exposed to atropine first were tested by EFS and the remaining purinergic force component is shown. (**F** and **G**) Representative traces of BSM purinergic contraction in response to EFS stimulation, which can be fully inhibited by adenylyl cyclase activators forskolin (n = 7) and NKH477 (n = 8), respectively. (**H** and **I**) Summarized data for **F** and **G,** respectively. (**J**) Dose response analyzed by nonlinear regression and IC_{50}.

$P2Y_{12}$ and A2b receptors are drug targets for the treatment of LUTS. Our data convincingly demonstrate that interplay between $P2Y_{12}$ and A2b signaling constitutes a central component of altered bladder function, indicating their potential to serve as attractive drug targets for treating LUTS. To test the viability of this hypothesis in vivo, A2b receptor agonist Bay 60-6583 was administrated to wild-type mice by i.p. injection; VSA was then performed and data were analyzed quantitatively. Provocatively, Bay 60-6583 dose-dependently increased PVS size and reduced PVS number. Bay 60-6583 started to take effect at 0.2 mg/kg, and by 1–2 mg/kg, increased the size of mouse PVS from approximately 350 mm^2 to greater than 500 mm^2, and reduced the PVS spot number from approximately 4 to 1–2 in 4 hours (Figure 7, A–D). Interestingly, Bay 60-6583 also reduced the total voiding area from mice (Figure 7E),

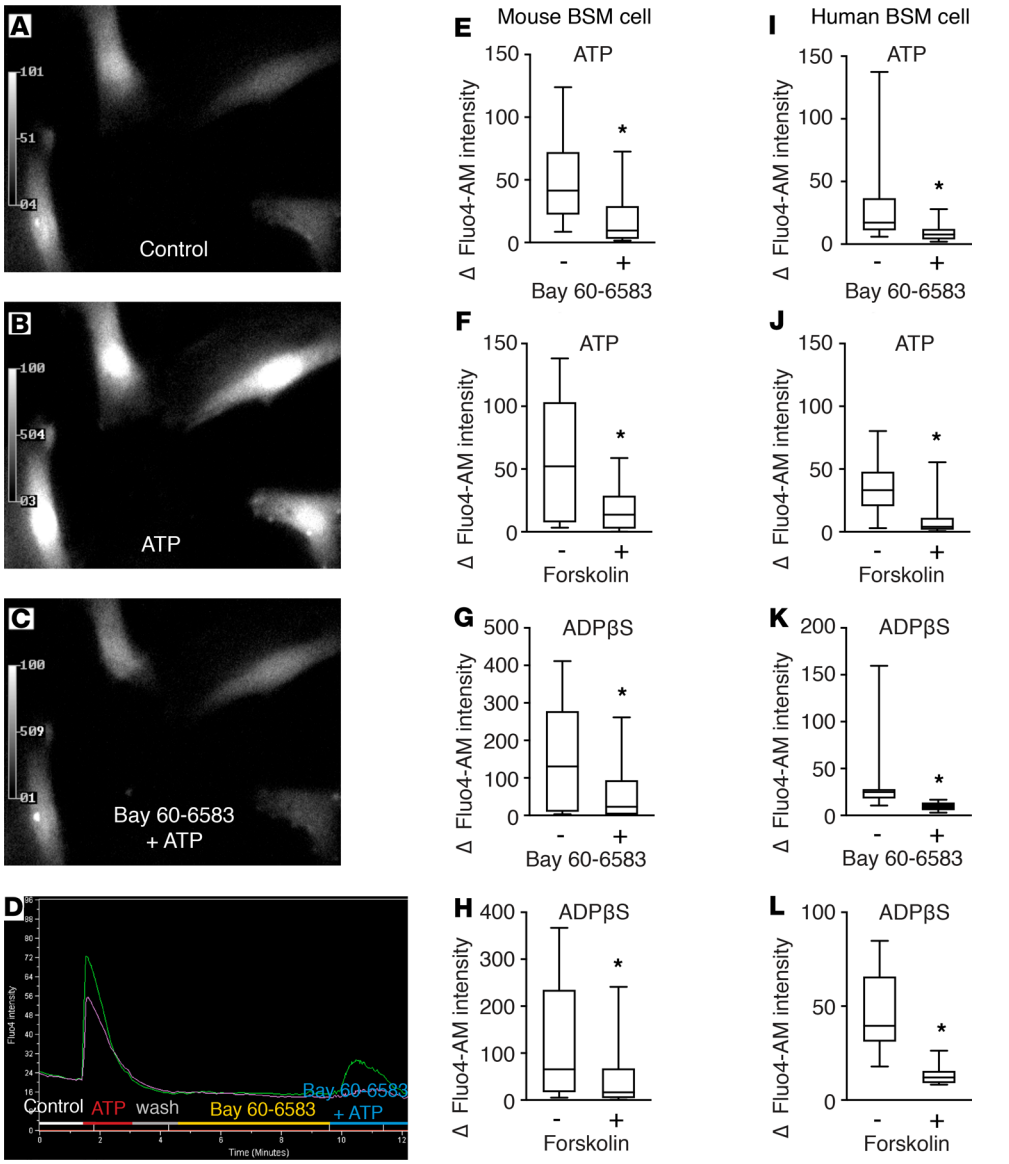

Figure 5. AC-cAMP signaling regulates bladder smooth muscle purinergic contractility through modulating downstream Ca^{2+} signaling in both mouse and human. (**A**) Representative image showing calcium-dependent fluorescence in control bladder smooth muscle (BSM) cells. The calcium signal is greatly enhanced by ATP (100 μM) or ADPβS (50 μM) stimulation as shown in **B**, and pretreatment of cells with A2b agonist Bay 60-6583 (1 μM) or forskolin (25 μM) abolishes the ATP or ADPβS stimulated effects (**C**). Quantitated data are shown in **E**–**L**. (**E**) $n = 17$, (**F**) $n = 10$, (**G**) $n = 24$, (**H**) $n = 27$, (**I**) $n = 20$, (**J**) $n = 24$, (**K**) $n = 13$, and (**L**) $n = 11$. Data are shown as box and whiskers, whiskers are from minimum to maximum, Student's *t* test is used to compare between drug-treated and untreated cells; $^*P < 0.05$.

suggesting that it might also increase water reabsorption in the kidney collecting duct and reduce the production of urine, an effect that could be particularly beneficial for patients with frequency and nocturia. To test this hypothesis, urine samples were collected and subjected to osmolality and chemical analysis. Interestingly, administration of Bay 60-6583 (2 mg/kg) resulted in a significant increase in urine osmolality (about 2-fold), consistent with reduced urine volume and in support of increased water reabsorption (Supplemental Figure 6B). Further chemical analysis indicated that urea concentration was significantly increased in urine from Bay 60-6583–treated mice (Supplemental Figure 6J). We were curious about whether this phenomenon also existed in $P2Y_{12}$- and A2b-deficient mice, and our data revealed some changes of osmolality and chemistry in these KO mice (Supplemental Figure 6), but further refined studies are needed to clearly understand their role in the regulation of kidney function.

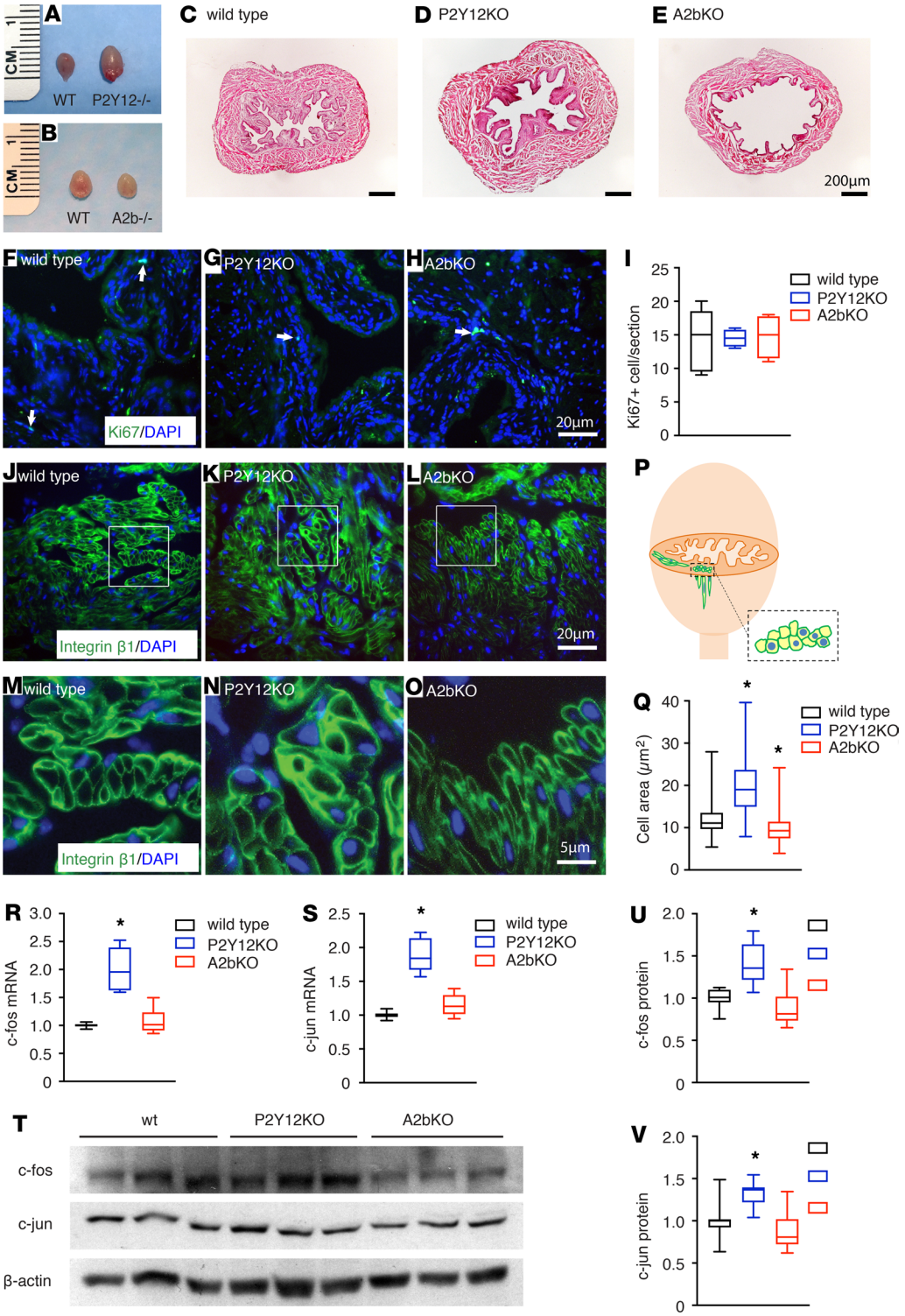

Figure 6. $P2Y_{12}$ and A2b signaling modulate bladder smooth muscle cell growth differentially through immediate early genes, c-fos and c-jun. Deletion of $P2Y_{12}$ and A2b result in enlarged (**A**) and reduced (**B**) bladder size, respectively. (**C**–**E**) H&E staining images from bladder sections of wild-type, $P2Y_{12}$-KO, and A2b-KO mice, respectively. (**F**–**H**) Immunostaining of Ki67 from bladder sections of wild-type (n = 5), $P2Y_{12}$-KO (n = 5), and A2b-KO (n = 5) mice, respectively. Positive nuclear staining per bladder section is quantitated in **I**. (**J**–**L**) Integrin β1 immunostaining of bladder sections of wild-type (n = 186 cells), $P2Y_{12}$-KO (n = 225 cells), and A2b-KO (n = 185 cells) mice, respectively. (**M**–**O**) Enlarged images of the white boxes seen in **J**, **K**, and **L**, respectively. (**P**) Schematic diagram indicating where the bladder was sectioned for staining, and how only bladder smooth muscle (BSM) cells containing nuclei were measured for their cross-section area, which serves as an index of BSM cell size. (**Q**) BSM cell cross-sectional area was quantitated for each model. (**R** and **S**) Quantitative RT-PCR data for *c-fos* and *c-jun* mRNA expression in mouse bladder from wild-type (n = 3), $P2Y_{12}$-KO (n = 3), and A2b-KO (n = 3) mice. (**T**) Western blot images of c-fos and c-jun protein expression in mouse bladder from wild-type (n = 6), $P2Y_{12}$-KO (n = 6), and A2b-KO (n = 6) mice, which are quantitated by densitometry and normalized to β-actin in **U** and **V**. Data are shown as box and whiskers, whiskers are from minimum to maximum, Student's t test is used to compare between wild-type and KO animals; $^*P < 0.05$.

As we noted above, deletion of $P2Y_{12}$ results in an UAB-like phenotype, and deletion of A2b causes an OAB-like phenotype; therefore, these KO mice themselves are strong models of OAB and UAB and will be useful for evaluating $P2Y_{12}$ and A2b receptors as drug targets for treating bladder disorders. In $P2Y_{12}$-KO mouse bladder, because of the lack of $P2Y_{12}$-mediated inhibition on AC-cAMP signaling, the A2b-mediated activation of AC-cAMP relaxation signaling will dominate (Figure 8). Therefore, to test whether we could rescue the UAB phenotype in $P2Y_{12}$-KO mice, we tested an A2b-receptor antagonist, PSB1115, by i.p. injections. Gratifyingly, PSB1115 dose-dependently reduced the size of PVSs and increased the number of PVSs in $P2Y_{12}$-KO mice by VSAs (Figure 7, F–J).

In the A2b-KO mouse, $P2Y_{12}$-mediated contraction signaling dominates (Figure 8). Therefore, we were highly motivated to test whether the OAB phenotype in these mice could be rescued pharmacologically, particularly because FDA-approved drugs for this receptor are available. Ticagrelor is a reversible $P2Y_{12}$ antagonist that was approved by the FDA in 2011 for prevention of thrombotic events in patients with acute coronary syndrome or myocardial infarction. Intriguingly, mice given i.p. injections of Ticagrelor dose-dependently increased the volume of their voids while simultaneously urinating less frequently (Figure 7, K–O). In sum, these data strongly indicate that targeted manipulation of smooth muscle contraction and relaxation by modulating the interplay of the $P2Y_{12}$ and A2b pathway can correct common LUTS-like symptoms.

Discussion

Purinergic or ATP-induced bladder contractility has been known for almost 50 years, and BSM was the very first tissue in which the concept of purinergic signaling was developed (41, 42). ATP is classically considered to exert its effects through $P2X_1$ receptors (8, 41, 42). Operating in parallel to the muscarinic receptor-dependent pathway, purinergic signaling plays an important role in initiating voiding function. However, this framework captures only a small part of the overall picture and says nothing about how bladder muscle relaxes and how it is regulated. In our previous work and in this study, we defined functional purinergic receptors $P2Y_{12}$ and A2b in BSM. We have shown that BSM purinergic contractility is defined mainly by the interplay of $P2X_1$, $P2Y_{12}$, and A2b-mediated pathways acting antagonistically through AC-cAMP regulated Ca^{2+} signaling (Figure 8). We have clearly shown that $P2Y_{12}$ and A2b receptors are important regulators of bladder activities, and deletion of $P2Y_{12}$ or A2b receptors result in opposing effects (UAB- or OAB-like phenotypes, respectively). We have thus extended our understanding greatly on how bladder muscle is regulated by purinergic signaling. These findings are important not just for understanding normal physiology of this tissue but they also offer potentially new therapeutic approaches to bladder dysfunctions, in which it is worth noting that upregulated purinergic signaling is commonly observed. As mentioned previously, antimuscarinic approaches show only marginal benefits in treating OAB (5), and chronic administration of oxybutynin induces a shift from muscarinic to purinergic transmission in the bladder wall of rats (6). Thus, drugs targeting this purinergic pathway will be of particular relevance in treating bladder dysfunctions. Our findings indicate that the opposing interplay of these receptors is predominantly restricted to effects on purinergic contractility and has little or no effect on muscarinic contractility. For example, A2b activation predominantly inhibits purinergic contraction induced by $P2X_1$ and $P2Y_{12}$ signaling. This finding is noteworthy because purinergic contractility is believed to be important in initiating voiding, whereas muscarinic contractility is important to maintain sustained contraction to expel the urine. We can therefore expect that drugs that inhibit purinergic contractility by A2b activation or $P2Y_{12}$ antagonism will likely delay voiding initiation and increase the urine volume, as was shown in our KO mice and drug treatment studies in mice (Figures 3 and 7). Conversely, because it does not interfere with muscarinic contractility directly, we can anticipate that the urine will be expelled completely, thus avoiding urine retention problems (and constipation, etc.) which are common adverse effects for antimuscarinics or β_3 receptor agonists.

We have shown that pharmacological activation of the $P2Y_{12}$ receptor causes significant BSM contraction, whereas activation of the A2b receptor inhibits BSM purinergic contraction. Therefore, it might be expected that deletion of the $P2Y_{12}$ receptor should result in reduced purinergic contractility and overall bladder contractile force and deletion of the A2b receptor should increase purinergic contraction and overall bladder contractile force. However, in vivo CMGs (Figure 3) and BSM strip experiments in KO mice show the opposite. Deletion of the $P2Y_{12}$ receptor results in significantly larger BSM contractile force and deletion of the A2b receptor causes diminished contractile force (Figure 4). This seems counterintuitive;

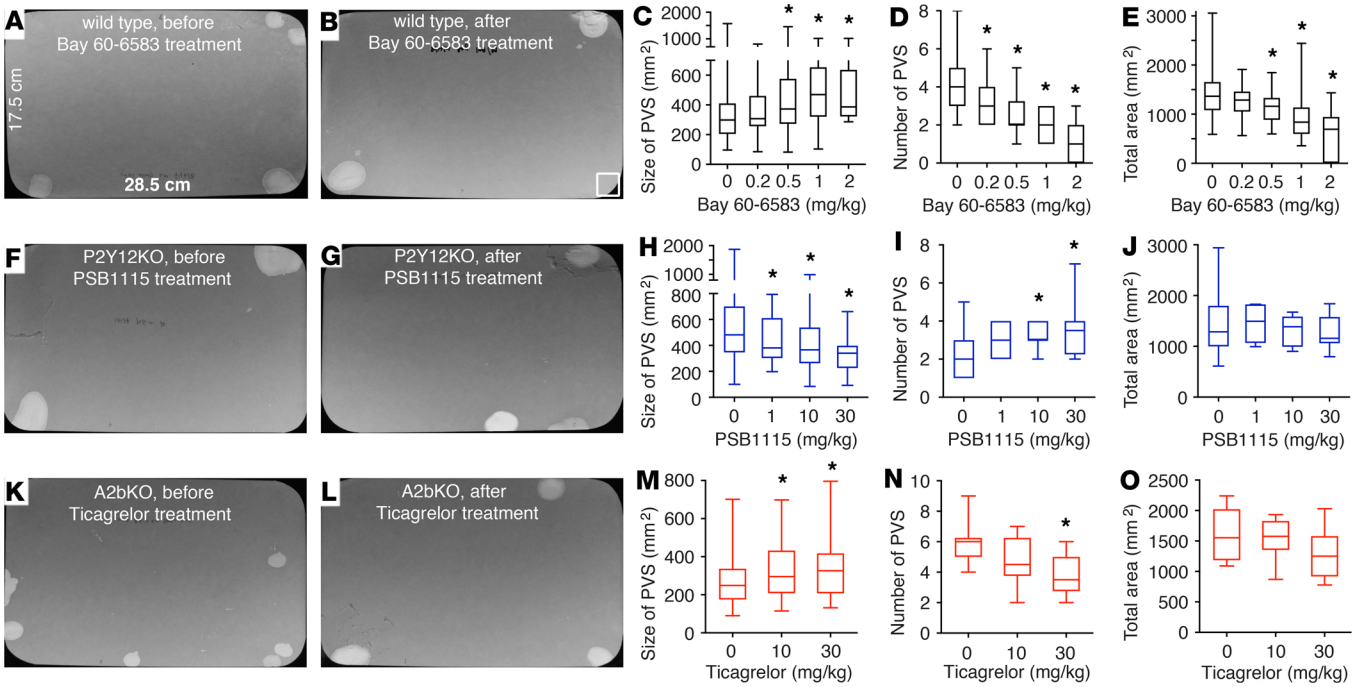

Figure 7. $P2Y_{12}$ and A2b receptors are drug targets for the treatment of lower urinary tract symptoms. (**A** and **B**) Representative images of voiding spot assay (VSA) filter papers from wild-type mice before (**A**) and after (**B**) Bay 60-6583 treatment. (**C**–**E**) Quantitated VSA data (n = 26). (**F** and **G**) Representative images of VSA filter papers from $P2Y_{12}$-KO mice before (**F**) and after (**G**) PSB1115 treatment. (**H**–**J**) Quantitated VSA data (n = 8). (**K** and **L**) Representative images of VSA filter papers from A2b-KO mice before (**K**) and after (**L**) Ticagrelor treatment. (**M**–**O**) Quantitated VSA data (n = 10). Data are shown as box and whiskers, whiskers are from minimum to maximum, 1-way ANOVA is used to examine the drug effect among groups, if significant, Student's t test is then used to compare between drug-treated and untreated groups; $^*P < 0.05$.

however, according to length-tension theory in muscle physiology, muscle needs to be elongated to an optimal length to generate maximal contractile force. Our data therefore suggest that activation of $P2Y_{12}$ signaling increases muscle tension and thus reduces muscle elongation, whereas activation of A2b signaling relaxes muscle and thus increases muscle length, resulting in paradoxical force outcomes. In $P2Y_{12}$-deleted mice (in which A2b signaling dominates, Figure 8), the muscle contractile force is significantly larger and the bladder capacity is also much bigger. The bladder is also more compliant with significantly higher peak pressures (Figures 3 and 4). However, in A2b-deleted mice (in which $P2Y_{12}$ signaling dominates, Figure 8), all parameters are the opposite (Figures 3 and 4).

Importantly, these data argue against the commonly held belief in urology that OAB is the result of too much contractile force, and thus drugs to treat OAB need to inhibit BSM contractile force. According to our findings, this dogma is overly simplistic because much more complicated mechanisms are at play (via length-tension optimization as a result of relaxation stimuli) in regulating bladder activity. In a CMG tracing, this could be colloquially summarized as "longer and stronger." Factors that increase BSM contractile force can actually result in increased bladder capacity and reduced bladder activity, whereas factors that decrease BSM contractile force can actually result in decreased capacity and overactivity as we have shown.

Deletion of the $P2Y_{12}$ or A2b receptor also results in significant remodeling of BSM. Our data indicate that proliferation seems unchanged in these bladders; however, intriguingly, there were significant differences in cell sizes (Figure 6). This altered cellular morphology could also play a role in our observed phenotypes. First, it could physically enlarge and reduce bladder size in $P2Y_{12}$-KO and A2b-KO mice, respectively, thus resulting in different bladder capacities in these KO mice. In addition, the larger BSM cells would presumably elongate further, perhaps resulting in greater capacity and higher contractile forces. The cell size difference is likely the result of different levels of cell growth. This is supported by our observation of changes in transcription factors c-fos and c-jun in $P2Y_{12}$- or A2b-deleted mice bladders. Because the bladder receives stretch force physiologically and pathologically, which can both induce substantial ATP/ADP/ADO release, these purinergic signals might play an important role in bladder remodeling that is commonly seen in bladder dysfunctions.

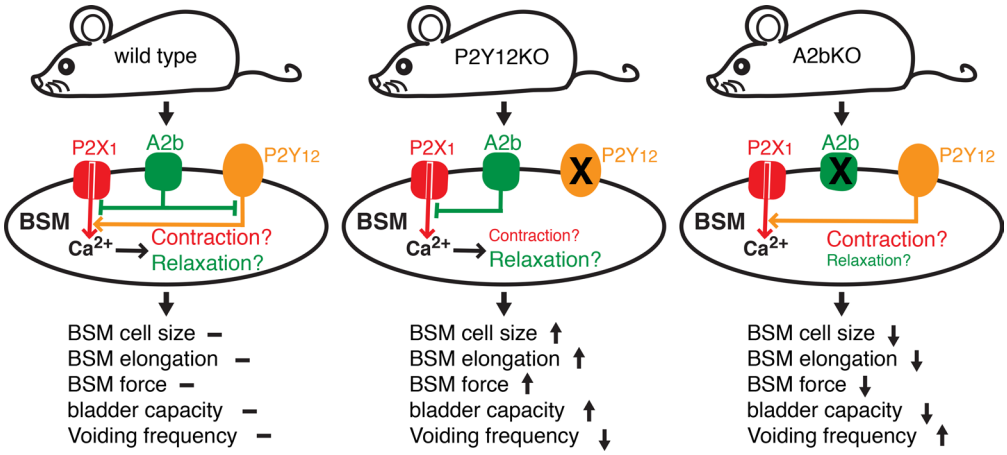

Figure 8. Feedforward and feedback interplay of $P2Y_{12}$ and A2b signaling plays a key role in regulating bladder smooth muscle cell function and overall bladder activity. $P2Y_{12}$ and A2b signaling oppositely modulate downstream AC-cAMP cascade and thus intracellular calcium signaling, which specifically regulates bladder smooth muscle (BSM) purinergic contractility. Regulation of this signaling is important for the status of BSM contraction and relaxation. When A2b signaling dominates as shown in $P2Y_{12}$-KO bladder, the relaxation activity will be dominant, resulting in increased bladder capacity and reduced voiding frequency. Conversely, when $P2Y_{12}$ signaling dominates as shown in A2b-KO bladder, the contracting activity will be dominant, resulting in decreased bladder capacity and increased voiding frequency.

Purinergic dysfunction is a common phenomenon in human bladder diseases; elevated ATP release, impaired ATP hydrolysis, and dysregulated P2X expression have all been reported in patients with OAB, interstitial cystitis, and outlet obstruction (16–18, 43–50). The role of $P2Y_{12}$ and A2b receptors in human bladder function is not well known. However, both $P2Y_{12}$ and A2B mRNA are well expressed in human bladder according to NCBI data. Interestingly, ADPβS has long been known to induce significant human BSM contraction, suggesting an important role of the $P2Y_{12}$ receptor in regulating human bladder activity (12, 22–24). Likewise, Northern blot and quantitative PCR analyses suggest high expression of A2b receptors in the human bladder wall (51, 52). Interestingly, the adenosine receptor antagonist caffeine can cause OAB, and caffeine ingestion leads to OAB, increased void frequency, and reduced volume per void (53, 54), suggesting an important role of the A2b receptor in regulating human bladder activity. Our findings in $P2Y_{12}$- or A2b-deleted mice bladders are consistent with these reports in human urological studies, suggesting a clear mechanism for OAB in human patients and indicating that both $P2Y_{12}$ and A2b are logical and appealing targets for treating human bladder disorders. Our pharmacological calcium imaging studies in primary cultured human BSM further support this claim (Figure 5). A2b receptor agonist Bay 60-6583 was proven to be potent in modulating in vivo mouse bladder function following i.p. injection (Figure 7). In addition, A2b receptor antagonist PSB1115 can reverse $P2Y_{12}$-KO mouse in vivo bladder function, and $P2Y_{12}$ receptor antagonist Ticagrelor can reverse A2b-KO mouse in vivo bladder function by single-dose injection (Figure 7). We predict these FDA-approved drugs, as well as currently unapproved drugs, are candidates that have great potential to readily translate into effective therapeutics for human patients with LUTS.

Methods

Reagents. Unless otherwise specified, all chemicals were obtained from MilliporeSigma and were of reagent grade or better. Agonists and antagonists, including α,β-Methyleneadenosine 5′-triphosphate trisodium (α,β-meATP), NECA, CGS21680, Bay 60-6583, Forskolin, and NKH 477 were all purchased from R&D Systems. Adenosine 5′-(β-thio)-diphosphate lithium salt (ADPβS) was purchased from Jena Bioscience. Fluo-4 AM, Pluronic F127, and X-gal were purchased from Invitrogen.

Animals. Male and female C57BL/6J mice (Jackson Laboratory), *$P2Y_{12}^{-/-}$* mice (55) in C57BL/6J background (provided by T.K. Gartner, University of Tennessee, Memphis, Tennessee, USA), and *$A2b^{-/-}$* mice (56) in C57BL/6J background (a gift from K. Ravid, Boston University, Boston, Massachusetts, USA) (aged 12–16 weeks) were used. All experiments and groups were performed under matching conditions for age and sex. Only male or female mice were used in some experiments (see below). If not specified, both male and female mice were used. Mice were euthanized by 100% CO_2 inhalation from a gas cylinder into a plexiglass chamber.

Myography. Bladders from male wild-type, *P2y*$_{12}^{-/-}$, and *A2b*$^{-/-}$ mice were pinned on a small Sylgard block and bladder mucosa was dissected away carefully. BSM strips were then cut longitudinally (2–3 mm wide and 5–7 mm long) and mounted in an SI-MB4 tissue bath system (World Precision Instruments). Force sensors were connected to a TBM 4M transbridge and the signal amplified by Powerlab and monitored through Chart software. Contraction force was monitored dynamically with a sampling rate of 2000/s. BSM strips were gently prestretched to get optimized force and equilibrated for at least 1 hour before any experiments. All experiments were conducted at 37°C in physiological saline solution (PSS in mM: Na, 136.9; K, 5.9; Ca, 2.5; Mg, 1.2; Cl, 133.6; HCO_3, 15.5; H_2PO_4, 1.2; glucose, 11.5; pH 7.4), with continuous bubbling of 95% O_2 and 5% CO_2. Data are analyzed statistically and BSM strip numbers are indicated as *n*.

EFS. EFS was carried out by a Grass S48 field stimulator (Grass Technologies) using standard protocols previously described (57).

Spontaneous VSA. VSAs were performed as described previously (58–60). Individual mice were gently placed in a standard polycarbonate mouse cage with Blicks Cosmos Blotting Paper (catalog 10422-1005) placed in the bottom, for 4 hours. Mice were given standard dry mouse chow for the duration of the assay. Water was withheld because of problems created by water dripping onto the filter paper. After 4 hours, the mice were returned to their home cages and the filter paper was allowed to dry. Filters were photographed under ultraviolet light at 365 nm in a UVP Chromato-Vue C-75 system (UVP) that incorporates an onboard Canon digital single lens reflex camera (EOS Rebel T3 – 12 megapixels). Overlapping voiding spots were visually examined and manually separated by outlining and copying, then pasting to a nearby empty space in Fiji software (http://fiji.sc/wiki/index.php/Fiji). Images were analyzed by UrineQuant software developed by us in collaboration with the Harvard Imaging and Data Core. The results table, which contains the area of each voiding spot and total number of spots, were imported into Excel software for further statistical processing. A volume/area standard curve on this paper determined that 1 mm^2 is equal to 0.283 μL urine. Voiding spots that have an area ≥80 mm^2 are considered to be PVSs (59, 60).

CMG. CMG was performed as described previously and only female mice were used in this experiment (58, 59). Mice were anesthetized by subcutaneous injection of urethane (1.4 g/kg). Once the pedal reflex was absent, a 1-cm midline abdominal incision was performed and a flame-flanged PE50 tubing was implanted through the dome of the bladder, which was secured in place with an 8-0 polypropylene surgical suture. The mouse was placed into a restrainer and the catheter was connected to a pressure transducer (and syringe pump by side arm) coupled to data acquisition devices (WPI Transbridge and AD Instruments Powerlab 4/35) and computerized recording system (AD Instruments LabChart software). Acquired data are analyzed and voiding interval, basal pressure, threshold pressure, changes of peak pressure, bladder compliance, and voiding interval are presented.

Mouse primary cultured BSM cell. Bladders from 4-week-old mice were retrieved aseptically. Bladder was cut into small pieces and digested in 1% collagenase (Gibco) at 37°C for 1 hour on a shaker. Digested cells were centrifuged down and resuspended in fresh DMEM medium with 10% FBS. The cells were seeded in a flask for 2 hours in 37°C, then transported to another new flask to discard the rapid adherent fibroblasts. Smooth muscle cells were ready for experiment after 4 to 5 days growth.

Human primary cultured BSM cell. Normal human BSM cell (catalog FC-0043) was purchased from LifeLine Cell Technology and cultured in VascuLife SMC culture medium (catalog LL-0014) with 5% FBS, 10 mM L-glutamine, 30 μg/mL ascorbic acid, and 5 ng/mL recombinant human EGF and FGF basic.

Calcium imaging. Primary cultured BSM cells seeded onto glass coverslips for 2 days were ready for calcium imaging (61). The cells were loaded with calcium sensitive dye FLUO4-AM (10 μM) and Pluronic F-127 (2.5 μg/mL) in the dark for 60 minutes. $[Ca^{2+}]_i$ was measured by exciting the cells at 495 nm light emitted from Lambda LS light source (Sutter Instrument). Images were digitized and analyzed using MetaFluor Imaging Software (Molecular Devices). The data were presented as fluorescence intensity. Drug application was regulated by VC-6 channel valve controller (Warner Instruments) and Peri-Star perfusion system (WPI).

RT-PCR and quantitative RT-PCR. Mouse bladders (wild type, *P2Y*$_{12}^{-/-}$, and *A2b*$^{-/-}$) were lysed for total RNA extraction by RNeasy Mini Kit (Qiagen). First-strand cDNA was synthesized from 1 μg total RNA using a SuperScript III First-Strand Synthesis System (Invitrogen). RT-PCR for gene detection and genotyping analysis was performed with Bio-Rad T100 Thermal Cycler. For quantitative RT-PCR, SYBR Green PCR Mix kits and a 7300 real-time PCR system (Applied Biosystems) was applied. SDHA (succinate dehydrogenase complex, subunit A) was used as an internal control. Each sample was analyzed triplicated. Primer details are provided in supplemental materials.

H&E staining. Frozen sectioned or paraffin-sectioned tissue was stained with Mayer's hematoxylin solution for 1 minute and rinsed with running water for 5 minutes before staining with Eosin Y Solution for 45 seconds. The slides were then rinsed shortly and dipped in 75%, 95%, 100% ethanol, and in xylene for 45 seconds, individually. Bladder tissue sections were protected in Permount mounting medium for imaging.

X-gal staining. The mice bladder tissue was fixed with 4% PFA for 1 hour at room temperature, placed in 30% sucrose for 2 hours at 4°C, then cryoprotected in OCT at –80°C. The tissue was frozen sectioned, washed with 1× PBS, and stained with X-gal staining solution (1 mg/mL X-gal, 5 mM $K_3Fe(CN)_6$, and 5 mM $K_3Fe(CN)$ $6H_2O$ in PBS) overnight at 37°C in the dark. The slides were then dipped in prewarmed X-gal washing buffer (0.1 M sodium phosphate, 2 mM $MgCl_2$, 0.01% sodium deoxycholate, and 0.02% NP-40) for several times, rinsed with PBS, and stained with H&E.

Western blot. Excised whole bladders were put in 0.5 mL ice-cold radio immunoprecipitation assay buffer (RIPA; 50 mM Tris pH 8.0, 150 mM NaCl, 1% v/v NP-40, 0.5% w/v deoxycholic acid, 0.1% w/v SDS) containing Complete Mini Protease Inhibitor Cocktail tablets (Roche). Proteins (15 μg/per lane) were resolved by SDS-PAGE (Tris-HEPES 8%–16% gel, catalog NH11-816; NuSep, GA) in Tris-HEPES running buffer (12.1 g Tris, 23.8 g HEPES, 1.0 g SDS, and H_2O to 1000 mL) at 120 constant voltage for 45–60 minutes, and then transferred to Immun-Blot PVDF membrane (BioRad Laboratories) in transfer buffer (Tris base 3.0 g, bicine 4.08 g, methanol 100 mL, and H_2O to 1000 mL) at 350 mA for 90–120 minutes at 4°C. The blots were blocked in 5% dehydrated milk in PBS overnight at 4°C, and then were probed with specific antibodies in 1% dehydrated milk in PBS for 2 hours at room temperature, followed by the appropriate species-specific secondary antibodies conjugated to HRP for 1 hour at room temperature. Three 15-minute washes were performed after the first and the secondary antibodies incubation with TBS Tween 20 (0.05%). Bands were detected using ECL Plus Western Blotting reagents (GE Healthcare) and CL-X Posure film (Thermo Scientific). The film was developed, scanned, and images were imported into Adobe Illustrator CS3. Protein bands were quantified by Fiji software and normalized to β actin signaling, and statistically analyzed. Details of antibodies used are provided in supplemental materials.

Immunofluorescence staining and microscopy imaging. Excised bladders were fixed in 4% (wt/vol) paraformaldehyde for 2 hours at room temperature. Fixed tissue was cryoprotected, frozen, sectioned, and incubated with rabbit polyclonal anti-Ki67 antibody (catalog ab15580, abcam) and purified rat anti-mouse β1 integrin antibody (catalog 550531, BD Bioscience) (1:100 dilution) overnight at 4°C. The sections were then incubated with Alexa Fluor 488–conjugated secondary antibody (diluted 1:100), and nuclei were stained with DAPI. Imaging was performed on an Olympus BX60 fluorescence microscope with a 40×/0.75 objective. Images (512 and 512 pixels) were saved as TIFF files and were imported into Adobe Illustrator CS3. In the current study, each bladder was sectioned to obtain 2 slides with approximately 4 sections of tissue on each slide. Each tissue section was examined under microscopy to ensure the consistency of the staining result, and images were taken and quantitated.

Statistics. Data are presented as mean ± SD. Data were analyzed using 2-tailed Student's *t* test for paired groups or 1-way ANOVA for comparison among groups. Bonferroni's multiple comparison post-hoc tests were used where necessary, and *P* values of less than 0.05 were considered to be significant.

Study approval. The Beth Israel Deaconess Medical Centre Institutional Animal Care and Use Committee approved these studies. Animals were used in adherence to NIH guidelines.

Author contributions

WY conceived the project. WY, YH, LW, and HC designed and performed the experiments. WY, YH, LW, and HC collected and analyzed data. WY, WGH, SCR, and MLZ contributed reagents/materials/analysis tools. WY, YH, LW, HC, WGH, SCR, and MLZ interpreted data and wrote the paper. All authors read and approved the final manuscript.

Acknowledgments

The authors acknowledge funding received from the US National Institute of Diabetes and Digestive and Kidney Diseases/National Institutes of Health grants DK-095922 (to WY). We thank Theodore K. Gartner for allowing us to use $P2Y_{12}$-KO mice in this study.

Address correspondence to: Weiqun Yu, Beth Israel Deaconess Medical Center, RN380B, 99 Brookline Avenue, Boston, Massachusetts 02215, USA. Phone: 617.667.5842; Email: wyu2@bidmc.harvard.edu.

1. Coyne KS, et al. The prevalence of lower urinary tract symptoms (LUTS) in the USA, the UK and Sweden: results from the Epidemiology of LUTS (EpiLUTS) study. *BJU Int*. 2009;104(3):352–360.
2. Irwin DE, Kopp ZS, Agatep B, Milsom I, Abrams P. Worldwide prevalence estimates of lower urinary tract symptoms, overactive bladder, urinary incontinence and bladder outlet obstruction. *BJU Int*. 2011;108(7):1132–1138.
3. Andersson KE, et al. The pharmacological treatment of urinary incontinence. *BJU Int*. 1999;84(9):923–947.
4. Yeaw J, Benner JS, Walt JG, Sian S, Smith DB. Comparing adherence and persistence across 6 chronic medication classes. *J Manag Care Pharm*. 2009;15(9):728–740.
5. Novara G, et al. A systematic review and meta-analysis of randomized controlled trials with antimuscarinic drugs for overactive bladder. *Eur Urol*. 2008;54(4):740–763.
6. Uvin P, et al. Chronic administration of anticholinergics in rats induces a shift from muscarinic to purinergic transmission in the bladder wall. *Eur Urol*. 2013;64(3):502–510.
7. Vial C, Evans RJ. P2X receptor expression in mouse urinary bladder and the requirement of P2X(1) receptors for functional P2X receptor responses in the mouse urinary bladder smooth muscle. *Br J Pharmacol*. 2000;131(7):1489–1495.
8. Heppner TJ, Werner ME, Nausch B, Vial C, Evans RJ, Nelson MT. Nerve-evoked purinergic signalling suppresses action potentials, Ca2+ flashes and contractility evoked by muscarinic receptor activation in mouse urinary bladder smooth muscle. *J Physiol (Lond)*. 2009;587(Pt 21):5275–5288.
9. Berridge MJ. Smooth muscle cell calcium activation mechanisms. *J Physiol (Lond)*. 2008;586(21):5047–5061.
10. Speakman MJ, Walmsley D, Brading AF. An in vitro pharmacological study of the human trigone--a site of non-adrenergic, non-cholinergic neurotransmission. *Br J Urol*. 1988;61(4):304–309.
11. Cowan WD, Daniel EE. Human female bladder and its noncholinergic contractile function. *Can J Physiol Pharmacol*. 1983;61(11):1236–1246.
12. Palea S, et al. ADP beta S induces contraction of the human isolated urinary bladder through a purinoceptor subtype different from P2X and P2Y. *J Pharmacol Exp Ther*. 1994;269(1):193–197.
13. Burnstock G. Purinergic signaling in the lower urinary tract. In: Abbracchio MP, Williams M, eds. *Handbook of Experimental Pharmacology*. Berlin, Germany: Springer Verlag; 2001:423–515.
14. Andersson KE, Arner A. Urinary bladder contraction and relaxation: physiology and pathophysiology. *Physiol Rev*. 2004;84(3):935–986.
15. Boselli C, Govoni S, Condino AM, D'Agostino G. Bladder instability: a re-appraisal of classical experimental approaches and development of new therapeutic strategies. *J Auton Pharmacol*. 2001;21(5-6):219–229.
16. Ouslander JG. Management of overactive bladder. *N Engl J Med*. 2004;350(8):786–799.
17. Palea S, Artibani W, Ostardo E, Trist DG, Pietra C. Evidence for purinergic neurotransmission in human urinary bladder affected by interstitial cystitis. *J Urol*. 1993;150(6):2007–2012.
18. Saito M, Kondo A, Kato T, Hasegawa S, Miyake K. Response of the human neurogenic bladder to KCl, carbachol, ATP and CaCl2. *Br J Urol*. 1993;72(3):298–302.
19. Sjögren C, Andersson KE, Husted S, Mattiasson A, Moller-Madsen B. Atropine resistance of transmurally stimulated isolated human bladder muscle. *J Urol*. 1982;128(6):1368–1371.
20. Nardi-Schreiber A, et al. Defective ATP breakdown activity related to an ENTPD1 gene mutation demonstrated using ^{31}P NMR spectroscopy. *Chem Commun (Camb)*. 2017;53(65):9121–9124.
21. Yu W, Robson SC, Hill WG. Expression and distribution of ectonucleotidases in mouse urinary bladder. *PLoS ONE*. 2011;6(4):e18704.
22. Burnstock G, Cusack NJ, Meldrum LA. Effects of phosphorothioate analogues of ATP, ADP and AMP on guinea-pig taenia coli and urinary bladder. *Br J Pharmacol*. 1984;82(2):369–374.
23. Wiklund NP, Gustafsson LE. Indications for P2-purinoceptor subtypes in guinea pig smooth muscle. *Eur J Pharmacol*. 1988;148(3):361–370.
24. Yu W, Sun X, Robson SC, Hill WG. ADP-induced bladder contractility is mediated by P2Y12 receptor and temporally regulated by ectonucleotidases and adenosine signaling. *FASEB J*. 2014;28(12):5288–5298.
25. Nicholls J, Hourani SM, Kitchen I. Characterization of P1-purinoceptors on rat duodenum and urinary bladder. *Br J Pharmacol*. 1992;105(3):639–642.
26. Ikeda Y, Wu C, Fry CH Role of P1-receptors in the contractile function of guinea-pig and human detrusor smooth muscle. *J Physiol (Lond)*. 2003(551):C9.
27. King JA, Huddart H, Staff WG. Purinergic modulation of rat urinary bladder detrusor smooth muscle. *Gen Pharmacol*. 1997;29(4):597–604.
28. Gopalakrishnan SM, et al. Functional characterization of adenosine receptors and coupling to ATP-sensitive K+ channels in Guinea pig urinary bladder smooth muscle. *J Pharmacol Exp Ther*. 2002;300(3):910–917.
29. Ma TC, Barco A, Ratan RR, Willis DE. cAMP-responsive element-binding protein (CREB) and cAMP co-regulate activator protein 1 (AP1)-dependent regeneration-associated gene expression and neurite growth. *J Biol Chem*. 2014;289(47):32914–32925.
30. Delghandi MP, Johannessen M, Moens U. The cAMP signalling pathway activates CREB through PKA, p38 and MSK1 in NIH 3T3 cells. *Cell Signal*. 2005;17(11):1343–1351.
31. Della Fazia MA, Servillo G, Sassone-Corsi P. Cyclic AMP signalling and cellular proliferation: regulation of CREB and CREM. *FEBS Lett*. 1997;410(1):22–24.
32. Petersen RK, et al. Cyclic AMP (cAMP)-mediated stimulation of adipocyte differentiation requires the synergistic action of Epac- and cAMP-dependent protein kinase-dependent processes. *Mol Cell Biol*. 2008;28(11):3804–3816.
33. Manna PR, Stocco DM. Crosstalk of CREB and Fos/Jun on a single cis-element: transcriptional repression of the steroidogenic acute regulatory protein gene. *J Mol Endocrinol*. 2007;39(4):261–277.
34. Activation of Immediate Early Genes by Drugs of Abuse. Technical review. Rockville, Maryland, June 3-4, 1991. *NIDA Res Monogr*. 1993;125:1–211.

35. Morgan JI, Curran T. Role of ion flux in the control of c-fos expression. *Nature*. 1986;322(6079):552–555.
36. Murphy TH, Worley PF, Baraban JM. L-type voltage-sensitive calcium channels mediate synaptic activation of immediate early genes. *Neuron*. 1991;7(4):625–635.
37. Sheng M, Greenberg ME. The regulation and function of c-fos and other immediate early genes in the nervous system. *Neuron*. 1990;4(4):477–485.
38. Sheng M, McFadden G, Greenberg ME. Membrane depolarization and calcium induce c-fos transcription via phosphorylation of transcription factor CREB. *Neuron*. 1990;4(4):571–582.
39. Ramachandran A, et al. FosB regulates stretch-induced expression of extracellular matrix proteins in smooth muscle. *Am J Pathol*. 2011;179(6):2977–2989.
40. Wegener JW, et al. An essential role of Cav1.2 L-type calcium channel for urinary bladder function. *FASEB J*. 2004;18(10):1159–1161.
41. Burnstock G, Satchell DG, Smythe A. A comparison of the excitatory and inhibitory effects of non-adrenergic, non-cholinergic nerve stimulation and exogenously applied ATP on a variety of smooth muscle preparations from different vertebrate species. *Br J Pharmacol*. 1972;46(2):234–242.
42. Burnstock G, Dumsday B, Smythe A. Atropine resistant excitation of the urinary bladder: the possibility of transmission via nerves releasing a purine nucleotide. *Br J Pharmacol*. 1972;44(3):451–461.
43. Burnstock G. Purinergic signalling in the urinary tract in health and disease. *Purinergic Signal*. 2014;10(1):103–155.
44. Harvey RA, Skennerton DE, Newgreen D, Fry CH. The contractile potency of adenosine triphosphate and ecto-adenosine triphosphatase activity in guinea pig detrusor and detrusor from patients with a stable, unstable or obstructed bladder. *J Urol*. 2002;168(3):1235–1239.
45. Westfall TD, Kennedy C, Sneddon P. The ecto-ATPase inhibitor ARL 67156 enhances parasympathetic neurotransmission in the guinea-pig urinary bladder. *Eur J Pharmacol*. 1997;329(2-3):169–173.
46. Westfall TD, Kennedy C, Sneddon P. Enhancement of sympathetic purinergic neurotransmission in the guinea-pig isolated vas deferens by the novel ecto-ATPase inhibitor ARL 67156. *Br J Pharmacol*. 1996;117(5):867–872.
47. Silva-Ramos M, et al. Impairment of ATP hydrolysis decreases adenosine A1 receptor tonus favoring cholinergic nerve hyperactivity in the obstructed human urinary bladder. *Purinergic Signal*. 2015;11(4):595–606.
48. Nardi-Schreiber A, et al. Defective ATP breakdown activity related to an ENTPD1 gene mutation demonstrated using ^{31}P NMR spectroscopy. *Chem Commun (Camb)*. 2017;53(65):9121–9124.
49. Koh SD, Lee H, Ward SM, Sanders KM. The mystery of the interstitial cells in the urinary bladder. *Annu Rev Pharmacol Toxicol*. 2018;58:603–623.
50. Lee H, Koh BH, Peri LE, Sanders KM, Koh SD. Purinergic inhibitory regulation of murine detrusor muscles mediated by PDGFRα+ interstitial cells. *J Physiol (Lond)*. 2014;592(6):1283–1293.
51. Pakzad M, Ikeda Y, McCarthy C, Kitney DG, Jabr RI, Fry CH. Contractile effects and receptor analysis of adenosine-receptors in human detrusor muscle from stable and neuropathic bladders. *Naunyn Schmiedebergs Arch Pharmacol*. 2016;389(8):921–929.
52. Stehle JH, Rivkees SA, Lee JJ, Weaver DR, Deeds JD, Reppert SM. Molecular cloning and expression of the cDNA for a novel A2-adenosine receptor subtype. *Mol Endocrinol*. 1992;6(3):384–393.
53. Kershen R, Mann-Gow T, Yared J, Stromberg I, Zvara P. Caffeine ingestion causes detrusor overactivity and afferent nerve excitation in mice. *J Urol*. 2012;188(5):1986–1992.
54. Lohsiriwat S, Hirunsai M, Chaiyaprasithi B. Effect of caffeine on bladder function in patients with overactive bladder symptoms. *Urol Ann*. 2011;3(1):14–18.
55. Foster CJ, et al. Molecular identification and characterization of the platelet ADP receptor targeted by thienopyridine antithrombotic drugs. *J Clin Invest*. 2001;107(12):1591–1598.
56. Yang D, et al. The A2B adenosine receptor protects against inflammation and excessive vascular adhesion. *J Clin Invest*. 2006;116(7):1913–1923.
57. Sibley GN. A comparison of spontaneous and nerve-mediated activity in bladder muscle from man, pig and rabbit. *J Physiol (Lond)*. 1984;354:431–443.
58. Yu W, et al. Spontaneous voiding by mice reveals strain-specific lower urinary tract function to be a quantitative genetic trait. *Am J Physiol Renal Physiol*. 2014;306(11):F1296–F1307.
59. Rajandram R, Ong TA, Razack AH, MacIver B, Zeidel M, Yu W. Intact urothelial barrier function in a mouse model of ketamine-induced voiding dysfunction. *Am J Physiol Renal Physiol*. 2016;310(9):F885–F894.
60. Chen H, Zhang L, Hill WG, Yu W. Evaluating the voiding spot assay in mice: a simple method with complex environmental interactions. *Am J Physiol Renal Physiol*. 2017;313(6):F1274–F1280.
61. Hao Y, et al. G protein-coupled estrogen receptor inhibits the P2Y receptor-mediated Ca(2+) signaling pathway in human airway epithelia. *Pflugers Arch*. 2016;468(8):1489–1503.